Nonlinear Dyn (2019) 98:269–282
https://doi.org/10.1007/s11071-019-05188-y

ORIGINAL PAPER

Quintic time-dependent-coefficient derivative nonlinear Schrödinger equation in hydrodynamics or fiber optics: bilinear forms and dark/anti-dark/gray solitons

Ting-Ting Jia · Yi-Tian Gao · Gao-Fu Deng · Lei Hu

Received: 11 June 2019 / Accepted: 8 August 2019 / Published online: 7 September 2019

Abstract Studies on the water waves contribute to the design of the related industries, such as the marine and offshore engineering, while the media with the negative refractive index can be applied as the carrier media in fiber optics. In consideration of the inhomogeneities of the media and nonuniformities of the boundaries in the real physical backgrounds, a quintic time-dependent-coefficient derivative nonlinear Schrödinger equation for certain hydrodynamic wave packets or medium with the negative refractive index is investigated in this paper. Bilinear forms and the N-soliton solutions with respect to the nonzero background, which are different from those in the existing studies, are derived under the certain constraints. Conditions for the dark/anti-dark/gray solitons are deduced due to the properties of the solitons derived via the asymptotic analysis. Effects of the dispersion coefficient $\lambda(t)$, self-steepening coefficient $\alpha(t)$, cubic nonlinearity $\mu(t)$ and quintic nonlinearity $\nu(t)$ on the interactions between the anti-dark and gray solitons under the certain condition are investigated. Interactions among the dark, anti-dark and gray solitons are discussed under two cases: when $\alpha(t)/\lambda(t)$ and $\mu(t)/\lambda(t)$ are the constants, whether the interaction is elastic or not depends on whether $\lambda(t)$, $\alpha(t)$ and $\mu(t)$ are the constants or the functions of t; when $\alpha(t)/\lambda(t)$ and $\mu(t)/\lambda(t)$ are related to t, if the velocity of the soliton is a periodic function of t, the propagation of the corresponding soliton is periodic and the corresponding interaction is inelastic. Interactions among the three/four solitons are described to be elastic or inelastic based on the changes in the velocities and waveforms of the three/four solitons after the interactions.

Keywords Hydrodynamics or fiber optics · Quintic derivative nonlinear Schrödinger equation · Bilinear forms and N-soliton solutions · Conditions for dark/anti-dark/gray solitons · Effects of the time-dependent coefficients

T.-T. Jia · Y.-T. Gao (✉) · G.-F. Deng · L. Hu
Ministry-of-Education Key Laboratory of Fluid Mechanics and National Laboratory for Computational Fluid Dynamics, Beijing University of Aeronautics and Astronautics, Beijing 100191, China
e-mail: gaoyt163@163.com

1 Introduction

Water waves are one of the most common phenomena in nature, the study of which helps the design of the related industries, such as the energy development, marine and offshore engineering, hydraulic engineering and mechanical engineering [1–23]. Media with the negative refractive index are among the carrier media in fiber optics and can be applied in the fabrications of the optical guiding elements in integrated circuit and bidirectional optical waveguide coupling devices [24–29]. References [30–45] have used the derivative nonlinear Schrödinger (DNLS) equations to model the nonlinear phenomena in some fluids, optical fibers and inhomogeneous plasmas.

In hydrodynamics, long waves have been governed by the Korteweg–de Vries equation in the shallow-water limit, whereas short waves, by the nonlinear Schrödinger equation in the deepwater limit, more precisely when $KH > 1.363$, where K is the carrier wavenumber and H is the unperturbed water depth [46,48]. However, through the combination of the asymptotic analysis and numerical simulations, in the framework of the higher-order DNLS equations with variable coefficients, it has been discovered that a wave packet in the deep water can penetrate into the shallow water ($KH < 1.363$) and propagate stably, depending on the initial value in deep water with a certain parameter related to the velocity of the wave packet [45]. It has been said that in the neighborhood of the "critical" $KH \approx 1.363$ [49], cubic nonlinearity weakens considerably, and higher-order nonlinear and dispersive effects need to be restored [48,50,51]. Higher-order, higher-dimensional, or even time-fractional DNLS equations have been introduced to describe the nonlinear phenomena in hydrodynamics [48,52–59].

With the uneven bottom into consideration so that H is allowed to be slowly varying with the space, a higher-order DNLS equation with time-dependent coefficients has been derived [45]. In the study of media with negative refractive index, negative permittivity and permeability have been considered [27,28]. Due to the inhomogeneities of media and nonuniformities of boundaries, time-dependent coefficients have been incorporated in the DNLS equations for describing the real physical backgrounds [29,42–45,47].

A quintic time-dependent-coefficient DNLS equation [42,43],

$$iu_t + \lambda(t)\, u_{xx} + i\alpha(t)\, |u|^2 u_x + \mu(t)\, |u|^2 u + \nu(t)\, |u|^4 u = 0, \tag{1}$$

has arisen in the study of hydrodynamic wave packets and media with the negative refractive index, where $u(x,t)$ is the wave envelope for the free water surface displacement or envelope of the electric field, t and x denote not only the propagation distance and retarded time in the context of optical fiber physics, but also the slow time and spatial coordinate traveling with the group velocity in hydrodynamics, while $\mu(t), \nu(t), \lambda(t)$ and $\alpha(t)$ represent the cubic nonlinearity, quintic nonlinearity, dispersion and self-steepening coefficients, respectively [42]. Additionally, special cases of Eq. (1) have been seen in the following:

– When $[\lambda(t), \alpha(t), \mu(t), \nu(t)] = [\hat{\lambda}, \hat{\alpha}, \hat{\mu}, \hat{\nu}]$, Eq. (1) has been reduced to a quintic DNLS equation describing the hydrodynamic wave packets and the medium with negative refractive index, where $\hat{\lambda}$, $\hat{\alpha}$, $\hat{\mu}$ and $\hat{\nu}$ are the constants [44,45]. Deformation and destruction of a water wave packet propagating shoreward from the deep to shallow water have been described [45]. Gray solitons on a continuous-wave background have been derived via two integrals of motion [44], and the explicit power series solutions, singular and dark solitons have been constructed [60].
– When $[\lambda(t), \alpha(t), \mu(t), \nu(t)] = [\frac{\alpha}{2}, 0, -\frac{q_1}{\alpha}, -\frac{q_2}{\alpha}]$, Eq. (1) has been reduced to the equation describing the Madelung fluid, where α, q_1 and q_2 are the constants [61]. Bright and gray/dark solitary waves are derived [61].
– When $[\lambda(t), \alpha(t), \mu(t), \nu(t)] = [-1, \kappa, 0, 0]$, Eq. (1) has been reduced to the Chen–Lee–Liu equation for the nonlinear optical pulses in a quadratic nonlinear crystal involving the self-steepening without any concomitant self-phase modulation, where κ is a constant [62]. When $\kappa = 1$, soliton, breather, multi-rogue wave and rational solutions have been constructed [41].

Bright and kink solitons for Eq. (1) have been derived via the trial equation method [37], and the N-soliton solutions for Eq. (1) have been constructed via the bilinear forms [43]. By the way, it has been demonstrated that: A dark soliton is a nonlocalized traveling wave formed as a result of nonlinear resonance of a bore with a periodic wave, and appears as an intensity dip in an infinitely extended constant background [63,64]; Anti-dark soliton exists in the form of a bright pulse on a nonzero continuous-wave background [65]; Gray soliton exists under the background plane, with its amplitude less than the high of the background plane [61]; Dark and anti-dark solitons coexist on the same background in the normal dispersion regime [40]. It has also been proved analytically that a random frequency shift of a dark soliton results in a time jitter $\sqrt{2}$ times lower than that from the bright solitons [66,67], i.e., the dark solitons are more resistant to the perturbations than the bright ones [40].

However, to our knowledge, the bilinear forms for Eq. (1) different from those in Ref. [43] and dark/anti-dark/gray solitons with the nonzero background for Eq. (1) have not been investigated. In Sect. 2, we will construct such bilinear forms, and derive the N-soliton solutions for Eq. (1) under certain conditions. In Sect. 3, properties of the two solitons will be derived via the asymptotic analysis. In Sect. 4, conditions for the dark, anti-dark and gray solitons will be derived. In Sect. 5, interactions between/among the anti-dark, gray and dark solitons, as well as the effects of $\alpha(t)$, $\lambda(t)$ and $\mu(t)$ on the interactions will be discussed under two cases. In Sect. 6, we will give the conclusions.

2 Bilinear forms and N-soliton solutions for Eq. (1)

Introducing the transformation $u = g/f$, we construct the bilinear forms for Eq. (1), which are different from those in Ref. [43], as follows

$$\left[iD_t + \lambda(t)D_x^2 + \frac{\chi_1(t)^2}{2\lambda(t)} + \chi_2(t)\right](g\cdot f) = 0, \tag{2a}$$

$$\lambda(t)D_x\left(f\cdot f^*\right) + \chi_1(t)|f|^2 - \frac{1}{2}i\alpha(t)|g|^2 = 0, \tag{2b}$$

$$\lambda(t)\, D_x^2\left(f\cdot f^*\right) + \chi_2(t)|f|^2 - \frac{1}{2}i\alpha(t)D_x\left(g\cdot g^*\right) - \left[\mu(t) - i\frac{\chi_1(t)}{4\lambda(t)}\alpha(t)\right]|g|^2 = 0, \tag{2c}$$

with the condition [43]

$$\alpha(t)^2 + 8\lambda(t)\nu(t) = 0, \tag{3}$$

where g and f are complex differentiable function with respect to x and t, g^* and f^*, respectively, denote the complex conjugate of f and g, $\chi_1(t)$ and $\chi_2(t)$ are the nonzero complex functions of t, the bilinear operators D_t and D_x are defined by [68]

$$D_x^{\iota}D_t^{\tau}(\Theta\cdot\Upsilon) = \left(\frac{\partial}{\partial x} - \frac{\partial}{\partial x'}\right)^{\iota}\left(\frac{\partial}{\partial t} - \frac{\partial}{\partial t'}\right)^{\tau}\Theta(x,t)\,\Upsilon\left(x',t'\right)\Big|_{t'=t,x'=x}, \tag{4}$$

$\Theta(x,t)$ is a differentiable function with respect to x and t, $\Upsilon(x',t')$ is a differentiable function with respect to the formal variables x' and t', while ι and τ are both the nonnegative integers.

Based on Bilinear Forms (2), the N-soliton solutions for Eq. (1) can be expressed as

$$u = \frac{g_N}{f_N}, \tag{5}$$

where N is a positive integer. Then, g_N and f_N in Eq. (5) are derived as

$$g_N = \mathcal{G}e^{i[\eta_1 x + m_1(t)]}, \quad f_N = \mathcal{F}e^{i[\eta_2 x + m_2(t)]} \tag{6}$$

with

$$\mathcal{G} = 1 + \sum_{n=1}^{N}\left[\sum G_{N_1,\ldots,N_n}\exp\sum_{\rho=1}^{n}\left(\theta_{N_\rho} + 2i\phi_{N_\rho}\right)\right],$$

$$\mathcal{F} = 1 + \sum_{n=1}^{N}\left[\sum F_{N_1,\ldots,N_n}\exp\sum_{\rho=1}^{n}\theta_{N_\rho}\right],$$

$$\theta_j = k_j x + \omega_j(t),\ G_{N_1,\ldots,N_n} = F_{N_1,\ldots,N_n}\prod_{\rho=1}^{n}\frac{G_{N_\rho}}{F_{N_\rho}},$$

$$F_{N_1,\ldots,N_n} = \prod_{\rho=1}^{n}F_{N_\rho}\times\prod_{1\le N_l,N_d\le n}^{N_l<N_d}H_{N_l,N_d},$$

$$\chi_1(t) = \frac{1}{2}i\left[\alpha(t) - 4\eta_2\lambda(t)\right],$$

$$\chi_2(t) = -\frac{1}{2}\left(2\eta_1 + \eta_2\right)\alpha(t) + \frac{\alpha(t)^2}{8\lambda(t)} + 4\eta_2^2\lambda(t) + \mu(t),$$

where

$$\omega_j(t) = k_j\int\left[2\left(\eta_2 - \eta_1\right)\lambda(t) - \alpha(t)\right]\mathrm{d}t \pm \frac{1}{2}\int\Lambda_j\mathrm{d}t,$$

$$m_1(t) = \frac{1}{2}\left(\eta_2 - 2\eta_1\right)\int\alpha(t)\mathrm{d}t + \int\mu(t)\mathrm{d}t + m_2(t) + \left(\eta_2^2 + 2\eta_1\eta_2 - \eta_1^2\right)\int\lambda(t)\mathrm{d}t,$$

$$F_j = \exp\left(2i\phi_j\right)\frac{\Lambda_j + 2k_j\left[\alpha(t) + ik_j\lambda(t)\right]}{\Lambda_j + 2k_j\left[\alpha(t) - ik_j\lambda(t)\right]}G_j,$$

$$H_{s,h} = \frac{\Lambda_s\Lambda_h + k_s k_h\left(8k_s k_j\lambda(t)^2 - \Gamma_{s,h}\right)}{\Lambda_s\Lambda_h - k_s k_h\Gamma_{s,h}},$$

$$\Lambda_j = \sqrt{k_j^2\left\{\Omega - 4\lambda(t)\left[k_j^2\lambda(t) + 2\mu(t)\right]\right\}},$$

$$\Gamma_{s,h} = \Omega + 4\lambda(t)\left[k_s k_h\lambda(t) - 2\mu(t)\right],$$

$$\Omega = \alpha(t)^2 + 4\left(2\eta_1 - 3\eta_2\right)\alpha(t)\lambda(t),$$

η_1, η_2 and k_j's are the real constants, G_j's are the complex constants, $\sum$ means a summation over all possible subscripts $\{N_1,\ldots,N_n\}$ chosen from the set $\{1,2,\ldots,N\}$ under the condition that $N_1 \le \cdots \le$

$N_\rho \le N_{\rho+1} \le \cdots \le N_n$, while ρ, j, s, h, l, d and N_j's are the integers.

Since $\omega_j(t)$s are the real functions, it is required that Λ_j's are real, i.e.,

$$\alpha(t)^2 + 4(2\eta_1 - 3\eta_2)\alpha(t)\lambda(t) - 4\lambda(t)^2 k_j^2 - 8\lambda(t)\mu(t) \ge 0. \tag{7}$$

Due to $\chi_1(t) \neq 0$ and $\chi_2(t) \neq 0$, N-Soliton Solutions (5) needs to satisfy that

$$\begin{aligned} &\alpha(t) - 4\eta_2\lambda(t) \neq 0, \\ &\frac{\alpha(t)^2}{8\lambda(t)} - \frac{1}{2}(2\eta_1 + \eta_2)\alpha(t) + 4\eta_2^2\lambda(t) + \mu(t) \neq 0. \end{aligned} \tag{8}$$

If $\chi_1(t) = 0$ or $\chi_2(t) = 0$, N-Soliton Solutions (5), respectively, need to satisfy that

$$\alpha(t) = 4\eta_2\lambda(t), \quad \text{or} \quad \mu(t) = 4\eta_2(\eta_1 - \eta_2)\lambda(t). \tag{9}$$

Under Constraints (7)–(9), the N-soliton solutions with the nonzero background for Eq. (1) can be expressed as N-Soliton Solutions (5), which are different from those in Ref. [43].

However, different from the above, when $\chi_1(t) = 0$ and $\chi_2(t) = 0$, i.e., $\alpha(t) = 4\eta_2\lambda(t)$ and $\mu(t) = 4\eta_2(\eta_1 - \eta_2)\lambda(t)$, the solutions given by N-Soliton Solutions (5) are still different from those in Ref. [43], although the bilinear forms are the same as those in Ref. [43], which is caused by the expansion forms of f_N and g_N, namely, Expressions (6).

3 Asymptotic analysis

When $N = 2$, we can obtain the two-soliton solutions for Eq. (1) as

$$u = \frac{g_2}{f_2} = e^{i[(\eta_1-\eta_2)x + m_1(t) - m_2(t)]} \frac{1 + G_1 e^{\theta_1 + 2i\phi_1} + G_2 e^{\theta_2 + 2i\phi_2} + G_{1,2} e^{\theta_1+\theta_2+2i(\phi_1+\phi_2)}}{1 + F_1 e^{\theta_1} + F_2 e^{\theta_2} + F_{1,2} e^{\theta_1+\theta_2}}. \tag{10}$$

Then, we can derive $|u|^2$ as

$$|u|^2 = \frac{1 + G_1 e^{\theta_1 + 2i\phi_1} + G_2 e^{\theta_2 + 2i\phi_2} + G_{1,2} e^{\theta_1+\theta_2+2i(\phi_1+\phi_2)}}{1 + F_1 e^{\theta_1} + F_2 e^{\theta_2} + F_{1,2} e^{\theta_1+\theta_2}} \frac{1 + G_1^* e^{\theta_1 - 2i\phi_1} + G_2^* e^{\theta_2 - 2i\phi_2} + G_{1,2}^* e^{\theta_1+\theta_2-2i(\phi_1+\phi_2)}}{1 + F_1^* e^{\theta_1} + F_2^* e^{\theta_2} + F_{1,2}^* e^{\theta_1+\theta_2}}. \tag{11}$$

Under $G_{1,2} \neq 0$, we assume that

$$k_1 > k_2 > 0 \quad \text{and} \quad \omega_2(t)/k_2 > \omega_1(t)/k_1. \tag{12}$$

If θ_1 is fixed, θ_2 can be expressed as $\theta_2 = \frac{k_2}{k_1}\theta_1 + k_2\left[\frac{\omega_2(t)}{k_2} - \frac{\omega_1(t)}{k_1}\right]$. When $t \to -\infty$, we have $e^{\theta_2} \to 0$; when $t \to +\infty$, we have $e^{-\theta_2} \to 0$. So we can derive

$$\begin{aligned} S_1^- = \lim_{\substack{t\to-\infty \\ (\theta_1 \text{ fixed})}} |u|^2 &= 1 - \left|\operatorname{sech}\left(\frac{\theta_1}{2} + \frac{1}{2}\ln F_1\right)\right|^2 \\ &\times \left[\left|\sin\left(\phi_1 - \frac{1}{2} i \ln G_1\right)\right|^2 - \frac{|1 - F_1|^2}{4|\sqrt{G_1}|^2}\right], \end{aligned} \tag{13a}$$

$$\begin{aligned} S_1^+ &= \lim_{\substack{t\to+\infty \\ (\theta_1 \text{ fixed})}} |u|^2 \\ &= 1 - \left|\operatorname{sech}\left(\frac{\theta_1}{2} + \frac{1}{2}\ln\left(F_1 H_{1,2}\right)\right)\right|^2 \\ &\times \left[\left|\sin\left(\phi_1 - \frac{1}{2} i \ln\left(G_1 H_{1,2}\right)\right)\right|^2 \right. \\ &\left. - \frac{|1 - F_1 H_{1,2}|^2}{4|\sqrt{G_1 H_{1,2}}|^2}\right], \end{aligned} \tag{13b}$$

where S_1^- and S_1^+ denote the asymptotic expressions for the soliton S_1 before and after the interaction, respectively.

If θ_2 is fixed, θ_1 can be expressed as $\theta_1 = \frac{k_1}{k_2}\theta_2 + k_1\left[\frac{\omega_1(t)}{k_1} - \frac{\omega_2(t)}{k_2}\right]$. When $t \to -\infty$, we have $e^{-\theta_1} \to 0$; when $t \to +\infty$, we have $e^{\theta_1} \to 0$. So we can derive

Table 1 Properties of the solitonic interaction for the two-dark-soliton solutions

Solitons S_j $(j=1,2)$	Widths W_j	Amplitudes $A_j^{\pm}$	Velocities $V_j^{\pm}$	Phase shifts Δ_j
S_1^-	$2\,\lvert k_1\rvert^{-1}$	$\lvert\Phi_1\rvert^{\frac{1}{2}}$	V_1	$\left\lvert\frac{1}{2}k_1^{-1}\ln H_{1,2}\right\rvert$
S_1^+	$2\,\lvert k_1\rvert^{-1}$	$\lvert\Psi_1\rvert^{\frac{1}{2}}$	$V_1+k_1^{-1}\Delta$	
S_2^-	$2\,\lvert k_2\rvert^{-1}$	$\lvert\Psi_2\rvert^{\frac{1}{2}}$	$V_2+k_2^{-1}\Delta$	$\left\lvert\frac{1}{2}k_2^{-1}\ln H_{1,2}\right\rvert$
S_2^+	$2\,\lvert k_2\rvert^{-1}$	$\lvert\Phi_2\rvert^{\frac{1}{2}}$	V_2	

$$
\begin{aligned}
S_2^- = &\lim_{\substack{t\to-\infty \\ (\theta_2\text{ fixed})}} |u|^2 \\
=&1-\left|\operatorname{sech}\left(\frac{\theta_2}{2}+\frac{1}{2}\ln\left(F_2H_{1,2}\right)\right)\right|^2 \\
&\times\left[\left|\sin\left(\phi_2-\frac{1}{2}i\ln\left(G_2H_{1,2}\right)\right)\right|^2\right. \\
&\left.-\frac{|1-F_2H_{1,2}|^2}{4|\sqrt{G_2H_{1,2}}|^2}\right],
\end{aligned}
\tag{14a}
$$

$$
\begin{aligned}
S_2^+ = &\lim_{\substack{t\to+\infty \\ (\theta_2\text{ fixed})}} |u|^2 = 1-\left|\operatorname{sech}\left(\frac{\theta_2}{2}+\frac{1}{2}\ln F_2\right)\right|^2 \\
&\times\left[\left|\sin\left(\phi_2-\frac{1}{2}i\ln G_2\right)\right|^2-\frac{|1-F_2|^2}{4|\sqrt{G_2}|^2}\right],
\end{aligned}
\tag{14b}
$$

where S_2^- and S_2^+ denote the asymptotic expressions for the soliton S_2 before and after the interaction, respectively.

Based on Expressions (13) and (14), the relevant properties of the two solitons during the interaction, including the widths W_j $(j=1,2)$, amplitudes $A_j^{\pm}$, velocities $V_j^{\pm}$ and phase shifts Δ_j, are listed in Table 1, where Φ_j, Ψ_j, V_j and Δ can be written as

$$
\begin{aligned}
\Phi_j =& \left|\sin\left(\phi_j-\frac{1}{2}i\ln G_j\right)\right|^2-\left|\cosh\left[\frac{\ln\left(-F_j\right)}{2}\right]\right|^2, \\
\Psi_j =& \left|\sin\left(\phi_j-\frac{1}{2}i\ln(G_jH_{1,2})\right)\right|^2 \\
&-\left|\cosh\left[\frac{\ln\left(-F_jH_{1,2}\right)}{2}\right]\right|^2, \\
V_j =& \alpha(t)+2(\eta_1-\eta_2)\lambda(t)-\frac{\Lambda_j}{2k_j} \\
&+i4k_j\lambda(t)^2\frac{[2k_j\alpha(t)\lambda(t)^{-1}+\Lambda_j\lambda(t)^{-1}]_t}{4k_j^4\lambda(t)^2+[2k_j\alpha(t)+\Lambda_j]^2},
\end{aligned}
$$

$$
\begin{aligned}
\Delta =& -\left[\ln(H_{1,2})\right]_t \\
=& 8\frac{4\lambda(t)\left[\lambda(t)'\mu(t)-\lambda(t)\mu(t)'\right]}{\left[4k_1^2\lambda(t)^2+k_1^{-2}\Lambda_1^2\right]\Lambda_1\Lambda_2k_1^{-2}k_2^{-2}\lambda(t)^{-1}} \\
&+8\frac{[2(\eta_1-3\eta_2)\lambda(t)+\alpha(t)]\left[\lambda(t)\alpha(t)'-\alpha(t)\lambda(t)'\right]}{\left[4k_1^2\lambda(t)^2+k_1^{-2}\Lambda_1^2\right]\Lambda_1\Lambda_2k_1^{-2}k_2^{-2}\lambda(t)^{-1}},
\end{aligned}
$$

where $(\bullet)'=\frac{\partial}{\partial t}(\bullet)$.

Without loss of generality, we consider the case of $\eta_1=-\eta_2=1$ and $\phi_j=\frac{\pi}{2}$ for illustrating the asymptotic expressions of the two-dark-soliton solutions for Eq. (1). When $\phi_j=\frac{\pi}{2}$, Φ_j and Ψ_j are reduced as

$$
\begin{aligned}
\Phi_j = \Psi_j =& \frac{\mathrm{Re}(G_j+F_j)}{2|G_j|} = \frac{2k_j^2\lambda(t)}{\sqrt{\mathrm{Re}(G_j)^2+\mathrm{Im}(G_j)^2}} \\
&\times\frac{2\mathrm{Re}(G_j)k_j^2\lambda(t)+\mathrm{Im}(G_j)\left[\Lambda_j+2k_j\alpha(t)\right]}{4k_j^4\lambda(t)^2+\left[\Lambda_j+2k_j\alpha(t)\right]^2},
\end{aligned}
\tag{15}
$$

where $\mathrm{Re}(\bullet)$ and $\mathrm{Im}(\bullet)$ denote the real and imaginary parts of the element $\bullet$, respectively.

Based on Table 1, we can observe $A_j^{\pm}$'s $(j=1,2)$, $V_j^{\pm}$'s and Δ_j's are related to t, while W_j's are constant. Besides, under $\Delta=0$ or $\Delta\neq0$, the properties of the two solitons S_j's have different situations.

Assuming that

$$
\frac{\alpha(t)}{\lambda(t)}=\rho_1,\quad \frac{\mu(t)}{\lambda(t)}=\rho_2,
\tag{16}
$$

where ρ_1 and ρ_2 are the proportional coefficients, and then we can obtain two cases according to $\Delta=0$ and $\Delta\neq0$ as follows:

Case 1. **ρ_1 and ρ_1 are the constant.**
In this case, $\Delta=0$, i.e., $\ln H_{1,2}=$ const. We can obtain $V_j^-=V_j^+$ and $A_j^-=A_j^+$, which implies that the velocity, amplitude and

Table 2 Conditions of the dark, anti-dark and gray solitons

Solitons S_j $(j=1,2)$	Anti-dark soliton	Dark soliton	Gray soliton
Conditions under $\Phi_j = \Psi_j$	$\Phi_j < 0$	$\Phi_j = 1$	$0 < \Phi_j < 1$

width of the soliton S_j are unchanged after the interaction except that there is a phase shift, while the interaction is elastic.

Case 2. **ρ_1 and ρ_2 are related to t.** In this case, $\Delta \neq 0$, i.e., $\ln H_{1,2} \neq$ const. We can observe $V_j^- \neq V_j^+$ and $A_j^- = A_j^+$, which implies that the velocity of the soliton S_j is changed after the interaction, while the interaction is inelastic.

Note that: Under Expressions (16) and Constraints (7)–(9), without loss of generality, setting $\eta_1 = -\eta_2 = 1$, we will investigate these situations under $\rho_1 \neq -4$ or $\rho_2 \neq -8$.

4 Conditions for the dark, anti-dark and gray solitons

According to $A_j^{\pm}$ in Table 1 and Eq. (15), we can obtain the dark, anti-dark and gray solitons under the different conditions listed in Table 2.

According to Constraint (7), we can obtain

$$|k_j| < \frac{1}{2}\sqrt{\rho_1^2 + 20\rho_1 - 8\rho_2} \text{ and } \rho_2 < \frac{5}{2}\rho_1 + \frac{1}{8}\rho_1^2. \tag{17}$$

Based on Table 2, expressions of the conditions of the dark, anti-dark and gray solitons are derived as follows:

– According to $\Phi_j = 1$, we can reduce the condition for the dark solitons as

$$\begin{aligned} &2k_j^2\lambda(t)\Big\{\mathrm{Im}(G_j)\Lambda_j + 2k_j\left[\mathrm{Im}(G_j)\alpha(t)\right.\\ &\quad\left.+k_j\mathrm{Re}(G_j)\lambda(t)\right]\Big\} - \sqrt{\mathrm{Im}(G_j)^2 + \mathrm{Re}(G_j)^2}\\ &\Big\{\left[\Lambda_j + 2k_j\alpha(t)\right]^2 + 4k_j^4\lambda(t)^2\Big\} = 0. \end{aligned} \tag{18}$$

– According to $\Phi_j < 0$, we can reduce the condition for the anti-dark solitons as

$$\begin{aligned} &\lambda(t)\Big\{\mathrm{Im}(G_j)\Lambda_j + 2k_j\left[\mathrm{Im}(G_j)\alpha(t)\right.\\ &\quad\left.+k_j\mathrm{Re}(G_j)\lambda(t)\right]\Big\} < 0. \end{aligned} \tag{19}$$

– According to $0 < \Phi_j < 1$, we can reduce the condition for the gray solitons as

$$\begin{aligned} &\lambda(t)\Big\{\mathrm{Im}(G_j)\Lambda_j + 2k_j\left[\mathrm{Im}(G_j)\alpha(t)\right.\\ &\quad\left.+k_j\mathrm{Re}(G_j)\lambda(t)\right]\Big\} > 0,\\ &2k_j^2\lambda(t)\Big\{\mathrm{Im}(G_j)\Lambda_j\\ &\quad+2k_j\left[\mathrm{Im}(G_j)\alpha(t) + k_j\mathrm{Re}(G_j)\lambda(t)\right]\Big\}\\ &\quad-\sqrt{\mathrm{Im}(G_j)^2 + \mathrm{Re}(G_j)^2}\\ &\quad\Big\{\left[\Lambda_j + 2k_j\alpha(t)\right]^2 + 4k_j^4\lambda(t)^2\Big\} < 0. \end{aligned} \tag{20}$$

According to the above discussion, the three types of solitons, including the dark, anti-dark and gray solitons, are derived under Conditions (18)–(20), as seen in Fig. 1.

5 Discussions

Under Constraints (7) and (8), according to N-Soliton Solutions (5), we will analyze the interactions between or among the solitons and illustrate the effects of $\lambda(t)$, $\alpha(t)$ and $\mu(t)$ on the interactions with Case 1 and 2, respectively.

5.1 Interactions between two solitons

- **ρ_1 and ρ_2 are the constants.**

Because ρ_1 and ρ_2 are constants, under $\Delta = 0$ and $\eta_1 = -\eta_2 = 1$, the velocity $V_j^{\pm} = V_j$ $(j=1,2)$, and V_j is reduced as

$$\begin{aligned} V_j &= \alpha(t) + 4\lambda(t)\\ &\quad-\frac{\mathrm{sign}(k_j)}{2}|\lambda(t)|\sqrt{\rho_1^2 + 20\rho_1 - 8\rho_2 - 4k_j^2}, \end{aligned} \tag{21}$$

which indicates that V_j's are related to ρ_1, ρ_2 and $\lambda(t)$. With other parameters fixed, we obtain that V_j is proportional to k_j whether under $k_j > 0$ or $k_j < 0$,

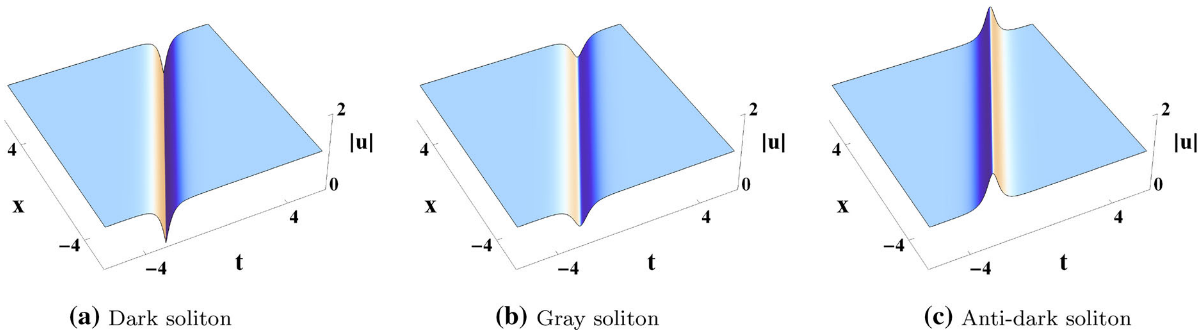

Fig. 1 Solitons via N-Soliton Solutions (5) under $N = 2$ with $-\alpha(t) = \lambda(t) = -\frac{1}{4}\mu(t) = 1$ and $k_1 = k_2 = 1.5$; **a** $G_1 = G_2 = 1$; **b** $G_1 = G_2 = 1 - i$; **c** $G_1 = G_2 = -1 + i$

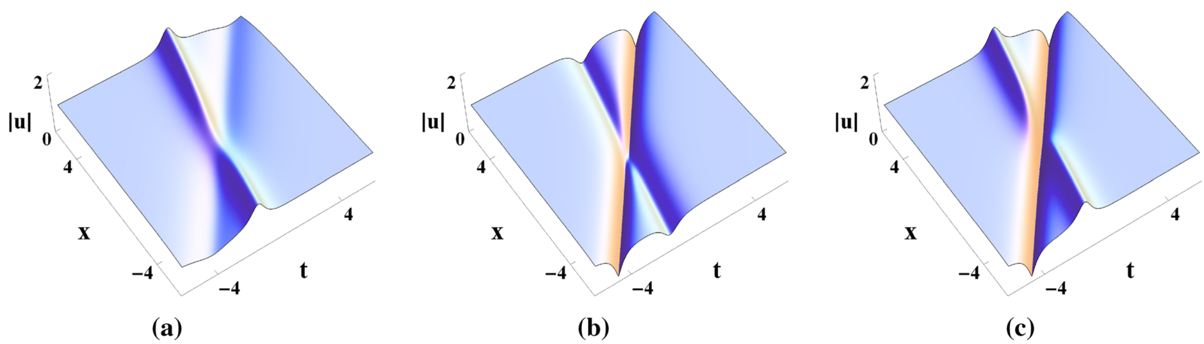

Fig. 2 Interactions between the two solitons via N-Soliton Solutions (5) under $N = 2$ with $-\alpha(t) = \lambda(t) = -\frac{1}{4}\mu(t) = 1$, $k_1 = -0.5$ and $k_2 = 0.6$; **a** interaction between the anti-dark and gray solitons with $G_1 = -1 + i$ and $G_2 = 1 - i$; **b** interaction between the dark and gray solitons with $G_1 = 1 - i$ and $G_2 = 1$; **c** interaction between the anti-dark and dark solitons with $G_1 = -1 + i$ and $G_2 = 1$

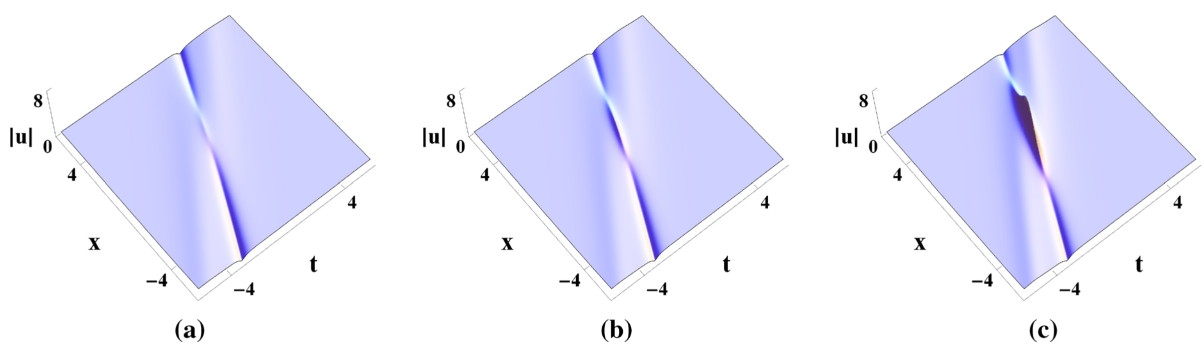

Fig. 3 Interactions between the gray and anti-dark solitons via N-Soliton Solutions (5) under $N = 2$ with $-\alpha(t) = \lambda(t) = -\frac{1}{4}\mu(t) = 1$, $G_1 = -1 + i$, $G_2 = 1$ and $k_2 = 1.5$; **a** $k_1 = 0.95$; **b** $k_1 = 1$; **c** $k_1 = 1.1$

whereas V_j under $k_j < 0$ is bigger than that under $k_j > 0$.

Under Conditions (18), (19) and (20), interactions, between the anti-dark and gray solitons, between the dark and gray solitons, as well as between the anti-dark and dark solitons, are described in Fig. 2a–c, respectively. We observe that V_j and Φ_j are invariable in Fig. 2 and the propagation of the soliton S_1 is faster than that of the soliton S_2 due to $V_1 > V_2$, which implies that the interactions are elastic.

Interactions between the gray and anti-dark solitons are described in Fig. 3. Amplitude in the interaction center increases with k_1 increasing. With V_2 unchanged, time of the interaction between the anti-

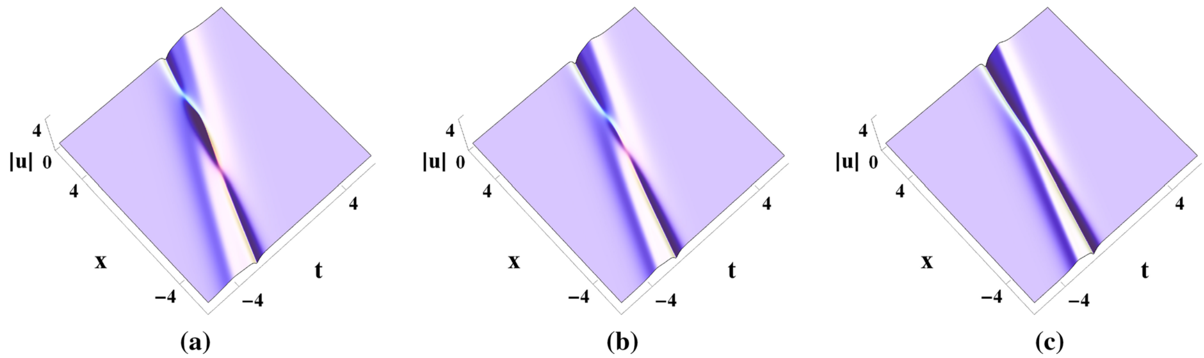

Fig. 4 Effects of $\lambda(t)$, with the same parameters as those in Fig. 3c except that **a** $\lambda(t) = 1.1$; **b** $\lambda(t) = 1.2$; **c** $\lambda(t) = 1.3$

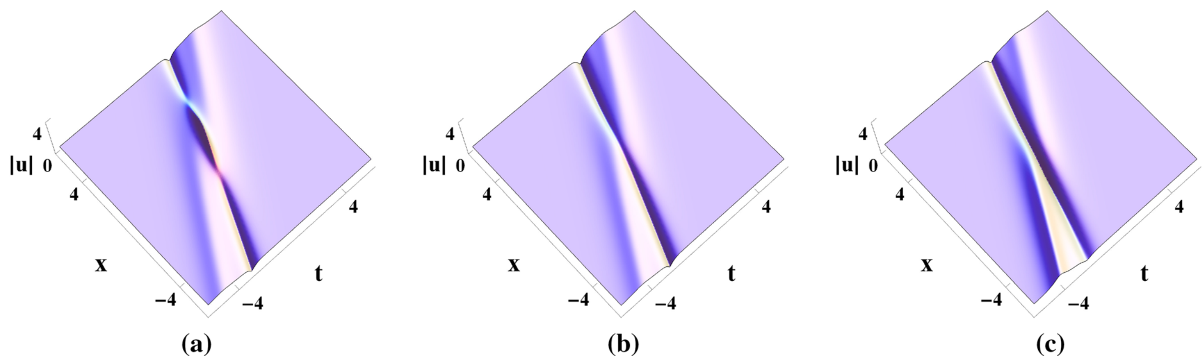

Fig. 5 Effects of $\alpha(t)$, with the same parameters as those in Fig. 3c except that **a** $\alpha(t) = -1.1$; **b** $\alpha(t) = -1.2$; **c** $\alpha(t) = -1.25$

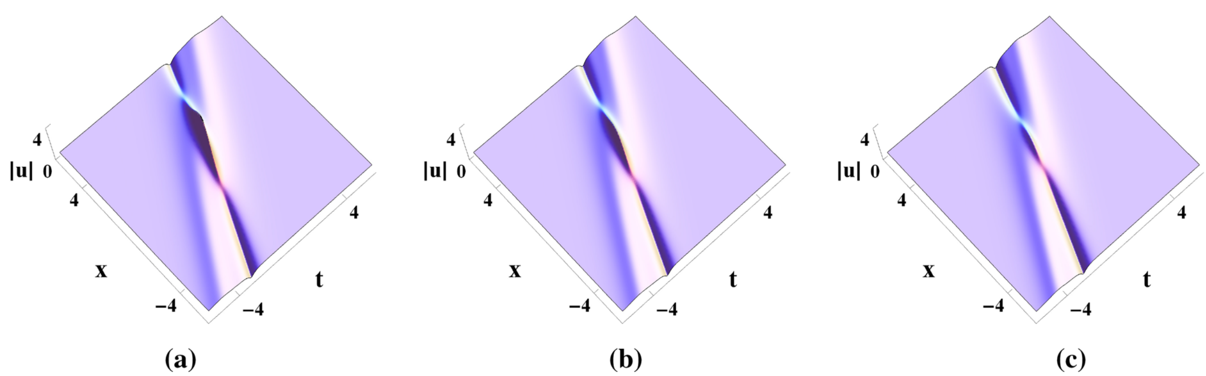

Fig. 6 Effects of $\mu(t)$, with the same parameters as those in Fig. 3c except that **a** $\mu(t) = -3.9$; **b** $\mu(t) = -3.8$; **c** $\mu(t) = -3.7$

dark soliton S_1 and gray soliton S_2 decreases as V_1 increases. Especially, under $k_1 = 1.1$ the amplitude is more than six times as high as the background.

Effects of $\lambda(t)$, $\alpha(t)$ and $\mu(t)$ on the interactions between the gray and anti-dark solitons are analyzed in Figs. 4, 5 and 6, respectively. According to Φ_j and V_j $(j = 1, 2)$, under $k_1 = 1.1$ and $k_2 = 1.5$, we observe that: the amplitude in the interaction center decreases not only as any one of $\mu(t)$ and $\lambda(t)$ increases, but also as $\alpha(t)$ decreases, whereas the amplitudes of the anti-dark and gray solitons increase not only as any one of $\lambda(t)$ and $\mu(t)$ increases, but also as $\alpha(t)$ decreases; V_j's are proportional to $\lambda(t)$ and $\mu(t)$, respectively, whereas V_j's decrease first and then increase with $\alpha(t)$ increasing.

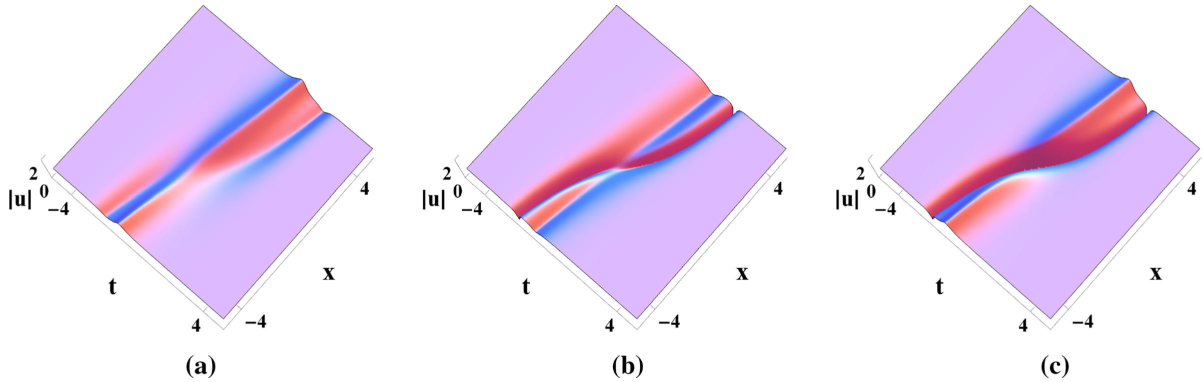

Fig. 7 The same as Fig. 2 except that $-\alpha(t) = \lambda(t) = -\frac{1}{4}\mu(t) = \cosh(t)$

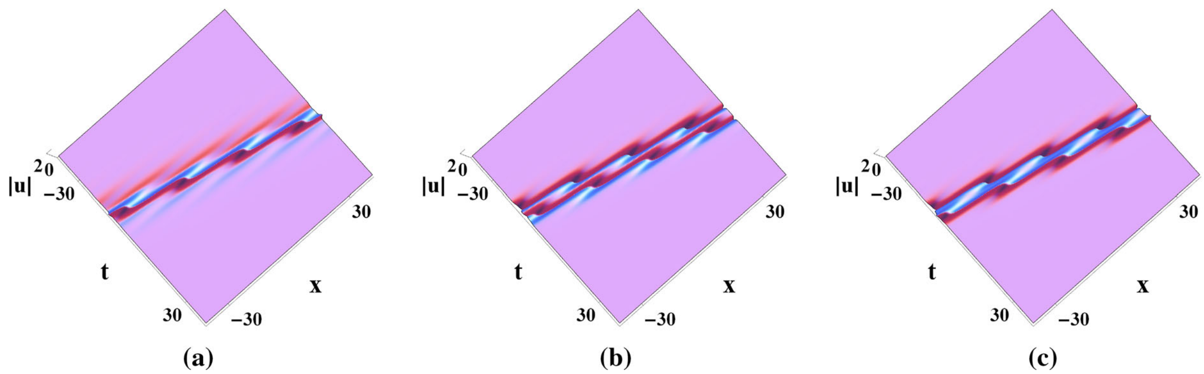

Fig. 8 The same as Fig. 2 except that $k_1 = 0.3$, $k_2 = 0.1$ and $\alpha(t) = \lambda(t) = \mu(t) = \cos(t) + 1.1$

When $\alpha(t)$, $\lambda(t)$ and $\mu(t)$ are real functions with respect to t, under $\rho_1 = -1$ and $\rho_2 = -4$, the interactions with $\lambda(t) = \cosh(t)$, between the anti-dark and dark solitons, between the gray and dark soliton, as well as between the anti-dark and gray solitons, are described in Fig. 7a–c, respectively. Under $\rho_1 = \rho_2 = 1$, interactions with $\lambda(t) = \cos(t) + 1.1$ are described in Fig. 8. Amplitude in the interaction center has a nonlinear superposition effect. According to Eq. (21), the velocities of the solitons in Figs. 7 and 8 are recorded as $V_{7,j}$ and $V_{8,j}$, respectively, as well as derived as

$$V_{7,j} = \cosh(t)\left[3 - \frac{1}{2}\mathrm{sign}(k_j)\sqrt{13 - 4k_j^2}\right],$$

$$V_{8,j} = \left[\cos(t) + \frac{11}{10}\right]\left[5 - \frac{1}{2}\mathrm{sign}(k_j)\sqrt{13 - 4k_j^2}\right].$$

Because $V_{7,j}$ and $V_{8,j}$ are the functions with respect to t, the interactions in Figs. 7 and 8 are inelastic. Especially, propagations of the two solitons in Fig. 8 have the periodicity due to $V_{8,j}$, while A_j's increase as $|t|$ increases in Fig. 8.

- **ρ_1 and ρ_2 are related to t.**

Because ρ_1 and ρ_2 are related to t, then $\Delta \neq 0$, and then $V_j^{\pm}$ and $A_j^{\pm}$ $(j = 1, 2)$ are more complex than that under the condition that ρ_1 and ρ_2 are constants, where V_j and Φ_j are rewritten as

$$\begin{aligned} V_j =& \alpha(t) + 4\lambda(t) \\ & - \frac{k_j|\lambda(t)|}{2|k_j|}\sqrt{\rho_1^2 + 20\rho_1 - 8\rho_2 - 4k_j^2} \\ & + \frac{ik_j\left[2k_j\rho_1 + \sqrt{\rho_1^2 + 20\rho_1 - 8\rho_2 - 4k_j^2}\right]_t}{4k_j^4 + \left[2k_j\rho_1 + \sqrt{\rho_1^2 + 20\rho_1 - 8\rho_2 - 4k_j^2}\right]^2}, \end{aligned} \tag{22a}$$

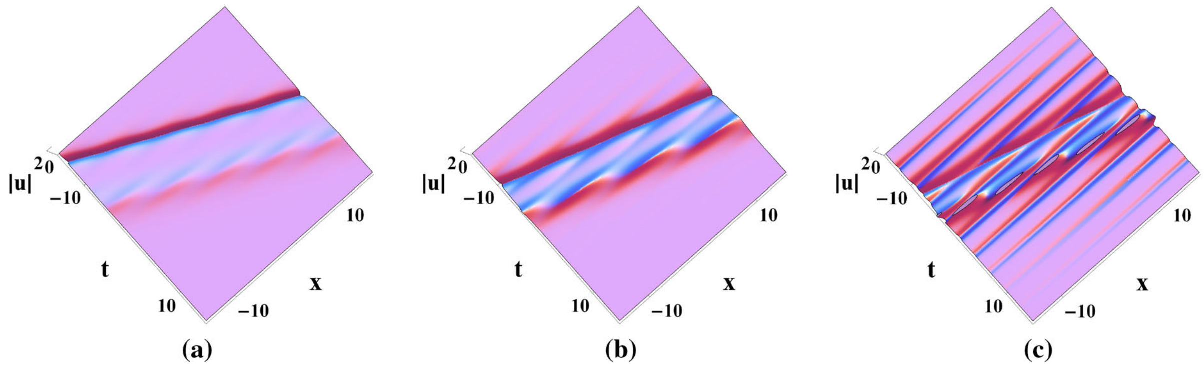

Fig. 9 Interactions between the anti-dark and dark solitons, with the same as Fig. 2c except that $k_1 = 0.3, k_2 = 0.1$ and $\alpha(t) = \lambda(t) = 1$; **a** $\mu(t) = -\cos^2(t) - 1.1$; **b** $\mu(t) = -\cos^2(t) + 1.1$; **c** $\mu(t) = \cos^2(t) + 1.1$

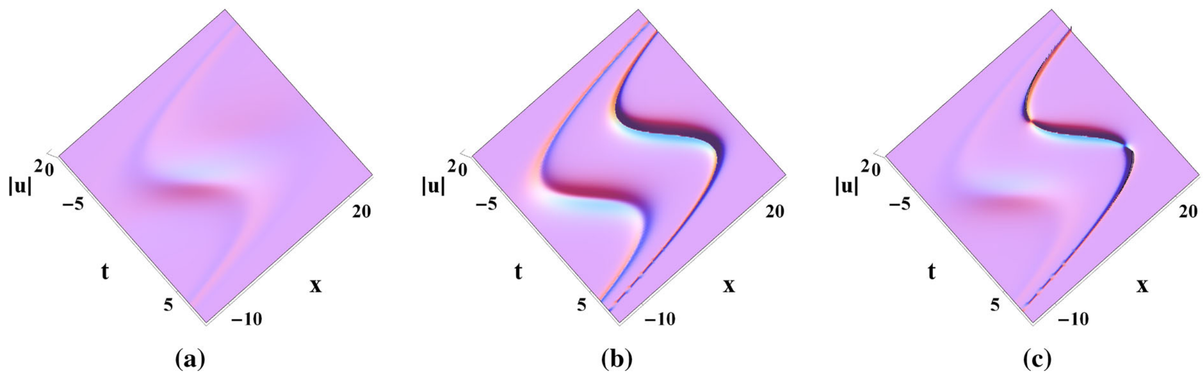

Fig. 10 The same as Fig. 2 except that $k_1 = 0.3, k_2 = 0.1, \alpha(t) = \lambda(t) = 1$ and $\mu(t) = -\cosh(t)$

$$\Phi_j = \frac{2k_j^2}{\sqrt{\mathrm{Re}(G_j)^2 + \mathrm{Im}(G_j)^2}} \times \left\{ \frac{\mathrm{Im}(G_j)\sqrt{\rho_1^2 + 20\rho_1 - 8\rho_2 - 4k_j^2}}{4k_j^4 + \left[2k_j\rho_1 + \sqrt{\rho_1^2 + 20\rho_1 - 8\rho_2 - 4k_j^2}\right]^2} + \frac{2k_j^2\mathrm{Re}(G_j) + 2k_j\rho_1\mathrm{Im}(G_j)}{4k_j^4 + \left[2k_j\rho_1 + \sqrt{\rho_1^2 + 20\rho_1 - 8\rho_2 - 4k_j^2}\right]^2} \right\}. \tag{22b}$$

According to Eq. (22), under $\rho_1 = 1$, when ρ_2 is a periodic function of t, V_j and A_j are the periodic functions of t, and the corresponding solitons propagate periodically. When ρ_2 increases from $-\cos^2(t) - 1.1$ to $-\cos^2(t) + 1.1$ and then to $\cos^2(t) + 1.1$, for the anti-dark and dark solitons, the corresponding V_j decreases in turn, whereas the corresponding Φ_j increases in turn, as seen in Fig. 9a–c.

Especially, when $\rho_1 = 1$ and $\rho_2 = -\cosh(t)$, the interactions between any two of the dark, anti-dark and gray solitons are described in Fig. 10. According to Eq. (22), we can observe that: when t tends to be infinite, Φ_j tends to be zero, whereas V_j tends to be infinite, which is affected by $\cosh(t)$.

5.2 Interactions among three or four solitons

Anti-dark, gray and dark solitons coexist on the nonzero background, as seen in Fig. 11. According to Φ_j and V_j, the waveforms and velocities of the anti-dark, gray and dark solitons all remain unchanged after the interaction, which indicates that the interaction is elastic, as seen in Fig. 11a, whereas the interactions in Fig. 11b, c are inelastic due to the changes with t of the waveforms and velocities of the solitons.

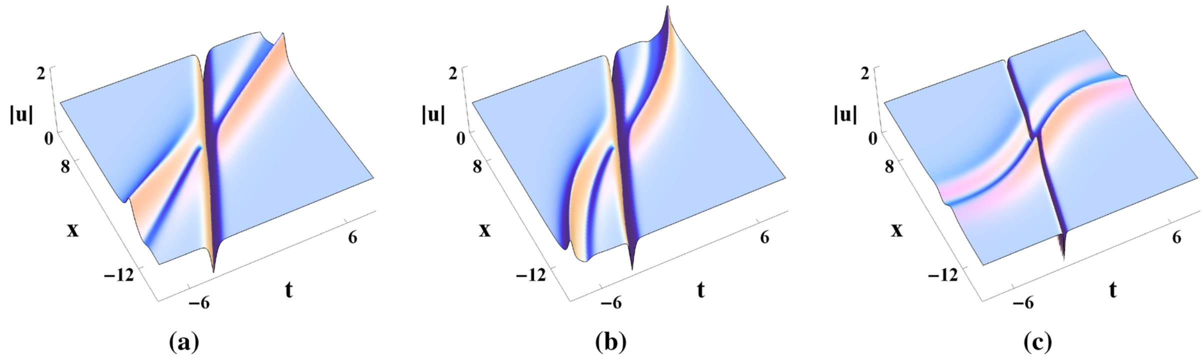

Fig. 11 Interaction among the dark, gray and anti-dark solitons via N-Soliton Solutions (5) under $N = 3$ with $-\alpha(t) = \lambda(t) = -\frac{1}{4}\mu(t) = 1$, $G_1 = 1$, $G_2 = 1 - i$, $G_3 = -1 + i$, $k_1 = 1.5$, $k_2 = -0.5$ and $k_3 = -1$; **a** $-\alpha(t) = \lambda(t) = -\frac{1}{4}\mu(t) = 1$; **b** $-\alpha(t) = \lambda(t) = -\frac{1}{4}\mu(t) = \cosh(\frac{t}{4})$; **c** $-\alpha(t) = \lambda(t) = \cosh(\frac{t}{4})$ and $\mu(t) = -4$

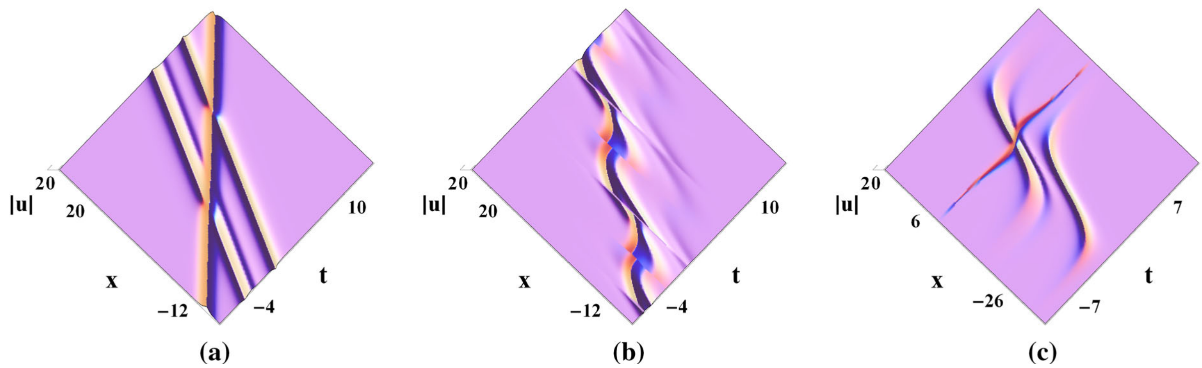

Fig. 12 Interactions among the dark, gray and anti-dark solitons via N-Soliton Solutions (5) under $N = 4$ with $G_1 = 1$, $G_2 = 1 - i$, $G_3 = -1 + i$, $G_4 = 1 - i$, $k_1 = 1.5$, $k_2 = -0.5$, $k_3 = -0.6$ and $k_4 = -0.4$; **a** $-\alpha(t) = \lambda(t) = -\frac{1}{4}\mu(t) = 1$; **b** $-\alpha(t) = \lambda(t) = -\frac{1}{4}\mu(t) = \cos(t) + 1.1$; **c** $\alpha(t) = \lambda(t) = \mathrm{sech}(t)$ and $\mu(t) = -4$

Under $N = 4$, interactions among the four solitons, including one gray soliton, one dark soliton and two anti-dark solitons, are described in Fig. 12. When $\rho_1 = \frac{1}{4}\rho_2 = -1$, then $\Delta = 0$, and then whether V_j's are invariable or variable depends on whether $\alpha(t)$ and $\lambda(t)$ are constants or functions of t, as seen in Fig. 12a, b, respectively. When $\rho_1 = 1$ and $\rho_2 = -4\cosh(t)$, then $\Delta \neq 0$, and then the interaction among the four solitons occurs on the nonzero background with $\alpha(t) = \lambda(t) = \mathrm{sech}(t)$, as seen in Fig. 12c.

6 Conclusions

Water waves are one of the most common phenomena in nature, while the media with negative refractive index are among the carrier media in fiber optics. Due to the inhomogeneities of the media and nonuniformities of the boundaries in the real physical backgrounds, a quintic DNLS equation with the time-dependent coefficients, i.e., Eq. (1), which describes certain hydrodynamic wave packets or medium with the negative refractive index, has been investigated. Under Constraints (7)–(9), we have derived Bilinear Forms (2) for Eq. (1), which are different from those in Ref. [43], and obtained N-Soliton Solutions (5) for Eq. (1) with respect to the nonzero background. Under Assumptions (12), properties of the two solitons, including the amplitudes $A_j^{\pm}$'s ($j = 1, 2$), velocities $V_j^{\pm}$'s, widths W_j's and phase shifts Δ_j's, have been derived via the asymptotic analysis and listed in Table 1. Conditions for the dark, anti-dark and gray solitons have been deduced in Table 2. Three types of the solitons have been described in Fig. 1.

Under Condition (3), quintic nonlinearity coefficient $\nu(t)$ has been demonstrated to be related to the dispersion coefficient $\lambda(t)$ and self-steepening coefficient $\alpha(t)$. Interactions between the two solitons and effects of $\alpha(t)$, $\lambda(t)$ and the cubic nonlinearity coefficient $\mu(t)$ on the interactions have been investigated under two cases:

Case 1, where $\frac{\alpha(t)}{\lambda(t)}$ and $\frac{\mu(t)}{\lambda(t)}$ are the constants.

- When $\alpha(t)$, $\lambda(t)$ and $\mu(t)$ are the constants, interactions, between any two of the dark, anti-dark and gray solitons, have been seen to be elastic, as seen in Fig. 2. Amplitude at the center of the interaction between the anti-dark and gray solitons has been found to increase not only with the decrease of $\alpha(t)$ but also with the increase of any of $\lambda(t)$, $\mu(t)$ and k_j, while $A_j^{\pm}$'s increase not only with the increase of $\alpha(t)$ but also with the decrease of any of $\lambda(t)$, $\mu(t)$ and k_j, as seen in Figs. 3, 4, 5 and 6.
- When $\alpha(t)$, $\lambda(t)$ and $\mu(t)$ are related to t, under $\frac{\alpha(t)}{\lambda(t)} = -1$ and $\frac{\mu(t)}{\lambda(t)} = -4$, we have found that: when $\lambda(t) = \cosh(t)$ or $\cos(t) + 1.1$, the interactions in Figs. 7 or 8 is inelastic due to the changes of $V_j^{\pm}$'s; propagation of the two solitons in Fig. 8 is periodic due to $\lambda(t) = \cos(t) + 1.1$.

Case 2, where $\frac{\alpha(t)}{\lambda(t)}$ and $\frac{\mu(t)}{\lambda(t)}$ are related to t.

- When $\frac{\alpha(t)}{\lambda(t)} = 1$, we have found that: When $\frac{\mu(t)}{\lambda(t)}$ increases from $-\cos^2(t) - 1.1$ to $-\cos^2(t) + 1.1$ and then to $\cos^2(t) + 1.1$, propagation of the two solitons remains periodic, while the corresponding V_j's decrease and A_j's increase, as seen in Fig. 9; when $\frac{\mu(t)}{\lambda(t)} = -\cosh(t)$, under $\lambda(t) = 1$, Φ_j tends to zero and V_j tends to the infinity as t tends to the infinity, which is affected by $\cosh(t)$, as seen in Fig. 10.

Anti-dark, dark and gray solitons have been found to coexist on the same nonzero background, as shown in Fig. 11; interactions among the three or four solitons have been investigated: when $\frac{\alpha(t)}{\lambda(t)} = -1$ and $\frac{\mu(t)}{\lambda(t)} = -4$, velocities and waveforms for the three solitons remain unchanged after the interaction under $\lambda(t) = 1$, indicating that the interaction in Fig. 11a is elastic, whereas the velocities for the three solitons change after the interaction under $\lambda(t) = \cosh(\frac{t}{4})$, indicating that the interaction in Fig. 11b is inelastic; under $\frac{\alpha(t)}{\lambda(t)} = -1$ and $\frac{\mu(t)}{\lambda(t)} = -4\mathrm{sech}(\frac{t}{4})$, interaction in Fig. 11c is inelastic due to the changes in the velocities for the solitons. Interaction is elastic in Fig. 12a due to the invariance of the waveforms and velocities for the four solitons, whereas interaction is inelastic in Fig. 12b, c due to the changes of the waveforms and velocities for the four solitons.

Acknowledgements We express our sincere thanks to the each member of our discussion group for their valuable suggestions. This work has been supported by the National Natural Science Foundation of China under Grant No. 11772017, and by the Fundamental Research Funds for the Central Universities under Grant No. 50100002016105010.

Compliance with ethical standards

Conflict of interest The authors declare that they have no conflict of interest.

References

1. Schneider, W., Yasuda, Y.: Stationary solitary waves in turbulent open-channel flow: analysis and experimental verification. J. Hydraul. Eng. **142**, 04015035 (2016)
2. Gao, X.Y.: Looking at a nonlinear inhomogeneous optical fiber through the generalized higher-order variable-coefficient Hirota equation. Appl. Math. Lett. **73**, 143–149 (2017)
3. Gao, X.Y.: Mathematical view with observational/experimental consideration on certain (2+1)-dimensional waves in the cosmic/laboratory dusty plasmas. Appl. Math. Lett. **91**, 165–172 (2019)
4. Li, Y.K., Wang, C.X., Liang, C.J., Li, J.D., Liu, W.A.: A simple early warning method for large internal solitary waves in the northern South China Sea. Appl. Ocean Res. **61**, 167–174 (2016)
5. Zhao, X.H., Tian, B., Guo, Y.J., Li, H.M.: Solitons interaction and integrability for a (2+1)-dimensional variable-coefficient Broer-Kaup system in water waves. Mod. Phys. Lett. B **32**, 1750268 (2018)
6. Zhao, X.H., Tian, B., Xie, X.Y., Wu, X.Y., Sun, Y., Guo, Y.J.: Solitons, Backlund transformation and Lax pair for a (2+1)-dimensional Davey-Stewartson system on surface waves of finite depth. Wave. Random Complex **28**, 356–366 (2018)
7. Benitz, M.A., Lackner, M.A., Schmidt, D.P.: Hydrodynamics of offshore structures with specific focus on wind energy applications. Renew. Sustain. Energy Rev. **44**, 692–716 (2015)
8. Yuan, Y.Q., Tian, B., Liu, L., Wu, X.Y., Sun, Y.: Solitons for the (2+1)-dimensional Konopelchenko-Dubrovsky equations. J. Math. Anal. Appl. **460**, 476–486 (2018)
9. Yuan, Y.Q., Tian, B., Chai, H.P., Wu, X.Y., Du, Z.: Vector semirational rogue waves for a coupled nonlinear Schrödinger system in a birefringent fiber. Appl. Math. Lett. **87**, 50–56 (2019)
10. Lu, X.: Madelung fluid description on a generalized mixed nonlinear Schrödinger equation. Nonlinear Dyn. **81**, 239–247 (2015)
11. Yin, H.M., Tian, B., Chai, J., Liu, L., Sun, Y.: Numerical solutions of a variable-coefficient nonlinear Schrödinger

equation for an inhomogeneous optical fiber. Comput. Math. Appl. **76**, 1827–1836 (2018)
12. Hu, Y.H., Zhu, Q.Y.: Dark and gray solitons of (2+1)-dimensional nonlocal nonlinear media with periodic response function. Nonlinear Dyn. **89**, 225–233 (2017)
13. Hu, C.C., Tian, B., Wu, X.Y., Du, Z., Zhao, X.H.: Lump wave-soliton and rogue wave-soliton interactions for a (3+1)-dimensional B-type Kadomtsev-Petviashvili equation in a fluid. Chin. J. Phys. **56**, 2395–2403 (2018)
14. Hu, C.C., Tian, B., Wu, X.Y., Yuan, Y.Q., Du, Z.: Mixed lump-kink and rogue wave-kink solutions for a (3 + 1)-dimensional B-type Kadomtsev-Petviashvili equation in fluid mechanics. Eur. Phys. J. Plus **133**, 40–47 (2018)
15. Wang, M., Tian, B., Sun, Y., Yin, H.M.: Zhang, Z: Mixed lump-stripe, bright rogue wave-stripe, dark rogue wave stripe and dark rogue wave solutions of a generalized Kadomtsev-Petviashvili equation in fluid mechanics. Chin. J. Phys. **60**, 440–449 (2019)
16. Wazwaz, A.M.: Abundant solutions of various physical features for the (2+1)-dimensional modified KdV–Calogero–Bogoyavlenskii–Schiff equation. Nonlinear Dyn. **89**, 1727–1732 (2017)
17. Du, Z., Tian, B., Chai, H.P., Yuan, Y.Q.: Vector multi-rogue waves for the three-coupled fourth-order nonlinear Schrödinger equations in an alpha helical protein. Commun. Nonlinear Sci. Numer. Simulat. **67**, 49–59 (2019)
18. Lu, X., Ma, W.X., Yu, J., Lin, F.H., Khalique, C.M.: Envelope bright- and dark-soliton solutions for the Gerdjikov–Ivanov model. Nonlinear Dyn. **82**, 1211–1220 (2015)
19. Chen, S.S., Tian, B., Sun, Y., Zhang, C.R.: Generalized darboux transformations, rogue waves, and modulation instability for the coherently coupled nonlinear Schrödinger equations in nonlinear optics. Ann. Phys. **531**, 1900011 (2019)
20. Lan, Z.Z.: Dark solitonic interactions for the (3+1)-dimensional coupled nonlinear Schrödinger equations in nonlinear optical fibers. Opt. Laser Technol. **113**, 462–466 (2019)
21. Lan, Z.Z., Hu, W.Q., Guo, B.L.: General propagation lattice Boltzmann model for a variable-coefficient compound KdV-Burgers equation. Appl. Math. Model. **73**, 695–714 (2019)
22. Zhang, C.R., Tian, B., Liu, L., Chai, H.P., Du, Z.: Vector breathers with the negatively coherent coupling in a weakly birefringent fiber. Wave Motion **84**, 68–80 (2019)
23. Du, X.X., Tian, B., Wu, X.Y., Yin, H.M., Zhang, C.R.: Lie group analysis, analytic solutions and conservation laws of the (3 + 1)-dimensional Zakharov-Kuznetsov-Burgers equation in a collisionless magnetized electron-positron-ion plasma. Eur. Phys. J. Plus **133**, 378–391 (2018)
24. Lazarides, N., Tsironis, G.P.: Superconducting metamaterials. Phys. Rep. **752**, 1–67 (2018)
25. Pazynin, L.A., Pazynin, V.L., Sliusarenko, H.O.: Negative refraction of plane electromagnetic waves in non-uniform double-negative media. Opt. Lett. **44**, 1125–1128 (2019)
26. Guo, R., Liu, Y.F., Hao, H.Q., Qi, F.H.: Coherently coupled solitons, breathers and rogue waves for polarized optical waves in an isotropic medium. Nonlinear Dyn. **80**, 1221–1230 (2015)
27. Golick, V.A., Kadygrob, D.V., Yampol'skii, V.A., Rakhmanov, A.L., Ivanov, B.A., Nori, Franco: Surface Josephson plasma waves in layered superconductors above the plasma frequency: evidence for a negative index of refraction. Phys. Rev. Lett. **104**, 187003 (2010)
28. Kivshar, Y.S., Shadrivov, I.V., Zharov, A.A., Ziolkowski, R.W.: Excitation of guided waves in layered structures with negative refraction. Opt. Express **13**, 481–492 (2005)
29. Marklund, M., Shukla, P.K., Stenflo, L.: Ultrashort solitons and kinetic effects in nonlinear metamaterials. Phys. Rev. E **73**, 037601 (2006)
30. Xu, S., Wang, L., Erdélyi, R., He, J.: Degeneracy in bright-dark solitons of the derivative nonlinear Schrödinger equation. Appl. Math. Lett. **87**, 64–72 (2019)
31. Li, M., Tian, B., Liu, W.J., Zhang, H.Q., Meng, X.H., Xu, T.: Soliton-like solutions of a derivative nonlinear Schrödinger equation with variable coefficients in inhomogeneous optical fibers. Nonlinear Dyn. **62**, 919–929 (2010)
32. Xu, T., Chen, Y.: Mixed interactions of localized waves in the three-component coupled derivative nonlinear Schrödinger equations. Nonlinear Dyn. **92**, 2133–2142 (2018)
33. Lü, X.: Soliton behavior for a generalized mixed nonlinear Schrödinger model with N-fold Darboux transformation. Chaos **23**, 033137 (2013)
34. Jenkins, R., Liu, J., Perry, P., Sulem, C.: Soliton resolution for the derivative nonlinear Schrödinger equation. Commun. Math. Phys. **363**, 1003–1049 (2018)
35. Khare, A., Cooper, F., Dawson, J.F.: Exact solutions of a generalized variant of the derivative nonlinear Schrödinger equation in a Scarff II external potential and their stability properties. J. Phys. A **51**, 445203 (2018)
36. Lü, X., Ma, W.X., Yu, J., Khalique, C.M.: Solitary waves with the Madelung fluid description: a generalized derivative nonlinear Schrödinger equation. Commun. Nonlinear Sci. Numer. Simul. **31**, 40–46 (2016)
37. Triki, H., Zhou, Q., Moshokoa, S.P., Ullah, M.Z., Biswas, A., Belic, M.: Gray and black optical solitons with quintic nonlinearity. Optik **154**, 354–359 (2018)
38. Grecu, D., Grecu, A.T., Visinescu, A.: Madelung fluid description of a coupled system of derivative NLS equations. Rom. J. Phys. **57**, 180–191 (2012)
39. Yu, W., Ekici, M., Mirzazadeh, M., Zhou, Q., Liu, W.J.: Periodic oscillations of dark solitons in nonlinear optics. Optik **165**, 341–344 (2018)
40. Li, M., Tian, B., Liu, W.J., Zhang, H.Q., Wang, P.: Dark and antidark solitons in the modified nonlinear Schrödinger equation accounting for the self-steepening effect. Phys. Rev. E **81**, 046606 (2010)
41. Zhang, Y.H., Guo, L.J., He, J.S., Zhou, Z.X.: Darboux transformation of the second-type derivative nonlinear Schrödinger equation. Lett. Math. Phys. **105**, 853–891 (2015)
42. Triki, H., Wazwaz, A.M.: A new trial equation method for finding exact chirped soliton solutions of the quintic derivative nonlinear Schrödinger equation with variable coefficients. Wave. Random Complex **27**, 153–162 (2017)
43. Jia, T.T., Gao, Y.T., Feng, Y.J., Hu, L., Su, J.J., Li, L.Q., Ding, C.C.: On the quintic time-dependent-coefficient derivative nonlinear Schrödinger equation in hydrodynamics or fiber optics. Nonlinear Dyn. **96**, 229–241 (2019)
44. Rogers, C., Chow, K.W.: Localized pulses for the quintic derivative nonlinear Schrödinger equation on a continuous-wave background. Phys. Rev. E **86**, 037601 (2012)

45. Grimshaw, R.H.J., Annenkov, S.Y.: Water wave packets over variable depth. Stud. Appl. Math. **126**, 409–427 (2011)
46. Ablowitz, M.J., Segur, H.: On the evolution of packets of water waves. J. Fluid Mech. **92**, 691–715 (1979)
47. Fedele, R., Schamel, H.: Solitary waves in the Madelung's fluid: connection between the nonlinear Schrödinger equation and the Korteweg–de Vries equation. Eur. Phys. J. B **27**, 313–320 (2002)
48. Slunyaev, A.V.: A high-order nonlinear envelope equation for gravity waves in finite-depth water. J. Exp. Theor. Phys. **101**, 926–941 (2005)
49. Benjamin, T.B., Feir, J.E.: The disintegration of wave trains on deep water. Part 1. J. Fluid Mech. **27**, 417–430 (1967)
50. Benilov, E.S., Flanagan, J.D., HOWLIN, C.P.: Evolution of packets of surface gravity waves over smooth topography. J. Fluid Mech. **533**, 171–181 (2005)
51. Johnson, R.S.: On the modulation of water waves in the neighbourhood of $kh \approx 1.363$. Proc. R. Soc. Lond. A **357**, 131–141 (1977)
52. Whitham, G.B.: Non-linear dispersion of water waves. J. Fluid Mech. **27**, 399–412 (1967)
53. Veeresha, P., Prakasha, D.G.: Solution for fractional Zakharov–Kuznetsov equations by using two reliable techniques. Chin. J. Phys. **60**, 313–330 (2019)
54. Veeresha, P., Prakasha, D.G.: New numerical surfaces to the mathematical model of cancer chemotherapy effect in Caputo fractional derivatives. Chaos **29**, 013119 (2019)
55. Veeresha, P., Prakasha, D.G.: A novel technique for (2+1)-dimensional time-fractional coupled Burgers equations. Math. Comput. Simul. **166**, 324–345 (2019)
56. Song, N., Zhang, W., Yao, M.H.: Complex nonlinearities of rogue waves in generalized inhomogeneous higher-order nonlinear Schrödinger equation. Nonlinear Dyn. **82**, 489–500 (2015)
57. Song, N., Zhang, W., Wang, P., Xue, Y.K.: Rogue wave solutions and generalized Darboux transformation for an inhomogeneous fifth-order nonlinear Schrödinger equation. J. Funct. space **2017**, 13 (2017)
58. Zhang, W., Wu, Q.L., Yao, M.H., Dowell, E.H.: Analysis on global and chaotic dynamics of nonlinear wave equations for truss core sandwich plate. Nonlinear Dyn. **94**, 21–37 (2018)
59. Zhang, W., Wu, Q.L., Ma, W.S.: Chaotic wave motions and chaotic dynamic responses of piezoelectric laminated composite rectangular thin plate under combined transverse and in-plane excitations. Int. J. Appl. Mech. **10**, 1850114 (2018)
60. Liu, W.H., Zhang, Y.F.: Optical soliton solutions, explicit power series solutions and linear stability analysis of the quintic derivative nonlinear Schrödinger equation. Opt. Quant. Electron. **51**, 65–77 (2019)
61. Fedele, R.: Envelope solitons versus solitons. Phys. Scr. **65**, 502–508 (2002)
62. Moses, J., Malomed, B.A., Wise, F.W.: Self-steepening of ultrashort optical pulses without self-phase-modulation. Phys. Rev. A **76**, 021802 (2007)
63. Emplit, P., Hamaide, J.P., Reinaud, F., Froehly, C., Bartelemy, A.: Picosecond steps and dark pulses through nonlinear single mode fibers. Opt. Commun. **62**, 374–379 (1987)
64. Il'ichev, A.T.: Envelope solitary waves and dark solitons at a water-ice interface. Proc. Steklov Inst. Math. **289**, 152–166 (2015)
65. Kivshar, Y.S.: Nonlinear dynamics near the zero-dispersion point in optical fibers. Phys. Rev. A **43**, 1677–1679 (1991)
66. Hamaide, J.P., Emplit, P., Haelterman, M.: Dark-soliton jitter in amplified optical transmission systems. Opt. Lett. **16**, 1578–1580 (1991)
67. Kivshar, Y.S., Haelterman, M., Emplit, P., Hamaide, J.P.: Gordon–Haus effect on dark solitons. Opt. Lett. **19**, 19–21 (1994)
68. Hirota, R., Nagai, A., Nimmo, J.J.C., Gilson, C.: The Direct Method in Soliton Theory. Cambridge University Press, Cambridge (2004)